Generation and characterization of the highest laser intensities (10^{22} W/cm²)

S.-W. Bahk, P. Rousseau, T. A. Planchon, V. Chvykov, G. Kalintchenko, A. Maksimchuk, G. A. Mourou, and V. Yanovsky

FOCUS Center and Center for Ultrafast Optical Science, University of Michigan, Ann Arbor, Michigan 48109-2099

We generated a record peak intensity of 0.7×10^{22} W/cm² by focusing a 45-TW laser beam with an $f/0.6$ off-axis paraboloid. The aberrations of the paraboloid and the low-energy reference laser beam were measured and corrected, and a focal spot size of 0.8 μm was achieved. It is shown that the peak intensity can be increased to 1.0×10^{22} W/cm² by correction of the wave front of a 45-TW beam relative to the reference beam. The phase and amplitude measurement provides for an efficient full characterization of the focal field. © 2004 Optical Society of America

OCIS codes: 010.1080, 140.3590, 320.7090.

The fundamental physics of high field laser–matter interactions (e.g., radiation reaction[1]) requires pushing the frontiers of laser intensity higher than the currently achieved level of 10^{21} W/cm².[2] At such high intensity, physical processes are poorly understood, and it is therefore desirable to have a well-characterized interacting electromagnetic field.

Generation of ultraintense light while it is simultaneously characterized with high spatial accuracy is a formidable proposition. First, to produce ultrahigh intensity it is more effective to obtain a tight focus than to increase laser power. However, tighter focusing is more readily affected by aberrations, so the method of correction without including the aberrations of a focusing optic[3] will not achieve a good result. Therefore we developed a new method with which to measure and correct the aberrations of a large-numerical-aperture focusing optic. The fact that we measure the phase after focusing leads us to an effective way to characterize the field. By use of a diffraction integral with measured phase and amplitude, the field, after focusing, can be calculated everywhere.[4] Such field calculations have occasionally been performed but with low accuracy because the aberrations of the focusing optics were not characterized.[5] The field calculation technique yields a more detailed analysis of the experimental results than spot size measurement or ionization.[6]

The application of tight focusing and aberration correction is shown schematically in Fig. 1(a). The 6.7 cm by 5.4 cm elliptical laser beam (attenuated regenerative amplifier beam) is focused by an $f/0.6$ paraboloid (7.62-cm diameter, 5.08-cm effective focal length, 90°). The all-Ti:sapphire laser (Hercules) essentially consists of a regenerative amplifier (40 mJ) and a four-pass amplifier followed by a two-pass amplifier (2.5 J before and 1.4 J after the compressor).[7] The power amplifiers exhibit minimal aberrations because the four-pass amplifier is cryogenically cooled and the two-pass amplifier is operated at a low repetition rate (0.1 Hz). The FWHM bandwidth at the regenerative amplifier level is 45 nm, and it becomes 43 nm at 30 TW. The autocorrelation trace of a 10-TW beam indicates a 30-fs pulse width that results from a Gaussian fit, where we have used a tilted-pulse-front single-shot autocorrelator.[8] The wave-

front aberrations are measured through an imaging system consisting of a field-curvature-corrected, apochromatic-infinity-corrected objective (40×; N.A., 0.75) and an achromatic lens ($f = 25$ cm). In detail, the objective forms a virtual image of the deformable mirror (DM) near the focus, and this image is relayed onto a Shack–Hartmann wave-front sensor (Imagine Optic) by an achromatic lens. The sensor has a 5 mm by 5 mm capture area of 8-bit dynamic range with a 32 by 32 microlenslet array. The focal length and the diameter of each microlens are 5.6 mm and 153 μm, respectively. The depth of focus is thus ~400λ, so the sensor is insensitive to a 45-nm bandwidth. As the diffraction effect is negligible from the DM to the paraboloid, the paraboloidal aberrations can be linearly added to the laser beam aberrations. This linearity allows us to directly control without further complications the wave-front distortion that is due either to the laser beam or the paraboloid. The DM was manufactured by Xinetics, Inc., and it consists of 96 actuators (lead magnesium niobate) controlling a 7.62-cm-diameter mirror surface by use of the electrostriction effect. The coating of the mirror (protected silver) can withstand as much as 300 mJ/cm² of energy density with 30-fs pulses. The maximum interactuator stroke is 2 μm. The
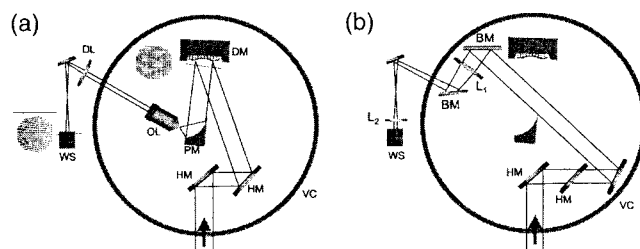
(a)   (b)

Fig. 1. (a) Experimental setup for measuring and correcting laser beam and focusing optic aberrations by use of a regen amplifier beam: HM, high-reflectivity mirror; DM, deformable mirror; PM, $f/0.6$ paraboloid; OL, infinity-corrected apochromatic–planatic objective with a N.A. of 0.75, 40×; DL, doublet lens; WS, Shack–Hartmann wave-front sensor; VC, vacuum chamber. (b) Setup for measuring the phase of a high-energy beam compared with that of a reference beam (regen beam): BM, blank mirror; L₁, lens, $f_1 = 50$ cm; L₂, lens, $f_2 = 4$ cm.

wave-front measurements before and after correction by the regenerative amplifier (regen) beam are shown in Figs. 2(a) and 2(b). The root-mean-square wave-front quality improved from 0.936λ to 0.066λ. A 12-bit camera image of the focal spot after wave-front correction is shown in Fig. 3(a). The FWHM spot size of the corrected focal spot is 0.8 μm, and the spatial resolution of the image is 40 pixels/μm. The main-lobe of the corrected spot in the 12-bit image contains approximately 60% of the total energy, whereas the calculated spot contains 80% [Fig. 3(b)]. The discrepancy can be attributed to the sensitivity to defocusing error of encircled energy of the experimental picture. In this tight focusing configuration, 1.5-μm defocusing results in 25% reduction in the encircled energy. The wave-front data shown are subject to two sources of error: statistical and measurement errors. The first is due to uncontrollable, random fluctuations of the wave front such as air turbulence and thermal drift in the amplifiers. The measurement errors are due to the finite sampling of the Shack–Hartmann sensor or to imperfect imaging in the wave-front measurement. The measurement errors in the imaging system [Fig. 1(a)] are estimated to be ~0.02λ rms. This estimation is based on the rms measurement of the wave front through a similar imaging system by use of a light source from a single-mode fiber tip. The sampling error is negligible because the analysis of a two-dimensional Fourier transform of the beam profile suggests a small number of high spatial frequency terms that are undetectable by the Shack–Hartmann sensor. Also, by inserting the attenuation filters we introduce nonnegligible first-order wave-front tilts as well as negligible higher-order terms (<0.015λ rms). The wave-front tilt errors have to be corrected with an external pointing system. We calculate the statistical rms values, however, by averaging the rms value of each wave front relative to the mean wave-front shape using 10–20 shots. The statistical rms values were 0.04λ at the regen and four-pass amplifier and 0.06λ at the two-pass amplifier level (>30 TW). The overall limit of the wave-front correction is determined by the statistical rms value, i.e., the shot-to-shot stability of the wave front. As these errors are small, the measured focal spot distributions match the calculated results well (Fig. 3).

After successfully achieving a wavelength-limited focal spot size with a low-energy reference beam (regen beam), we measured the higher-energy phase before focusing because we cannot use the objective owing to concerns about damage [Fig. 1(b)]. At this step, only the phase of a high-energy beam relative to that of the reference beam needs to be measured. To perform this measurement we took the transmitted part of a high-energy beam (45 TW) through a high-reflectivity mirror. The nonlinear effect through the reflector is negligible. In the relative measurement mode the aberrations in the imaging system were subtracted out. Figure 2(c) shows the phase of the 45-TW beam relative to that of the regen beam. The rms value is 0.154λ. As the high-power beam and the reference beam follow the same path and traverse the same optics, the total input field at high energy can be constructed by addition of the residual reference phase
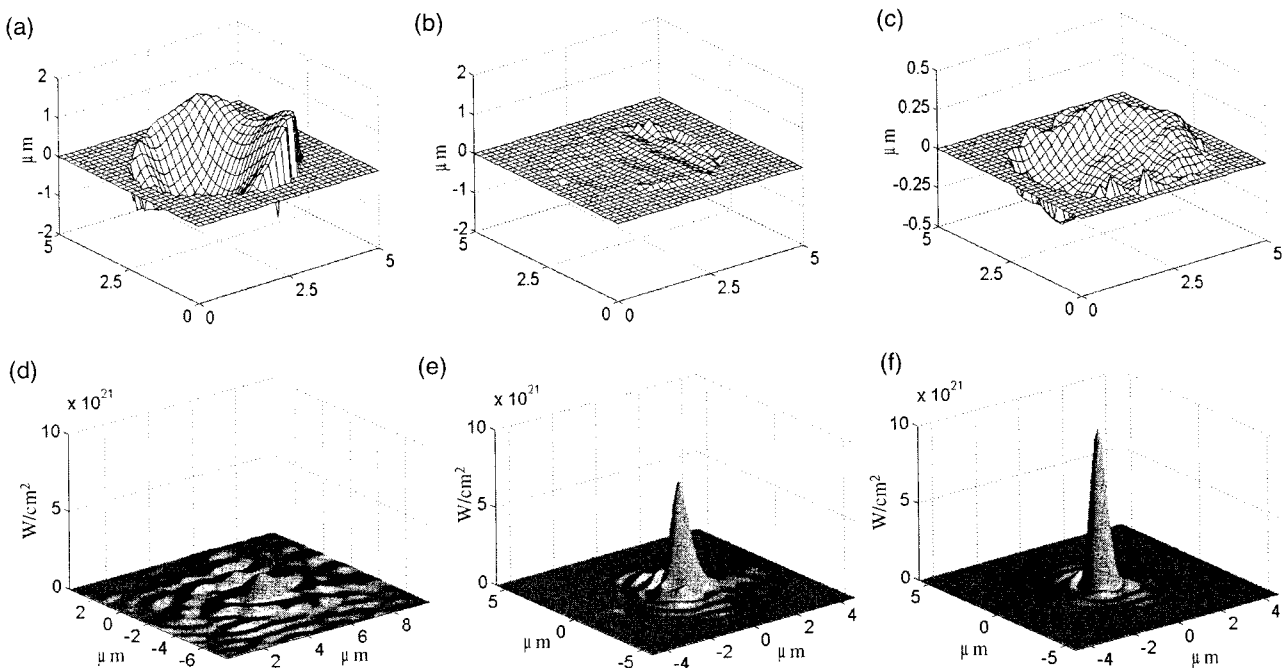

Fig. 2. (a)–(c) Measured wave fronts and (d)–(f) calculated focused intensities. (a) Wave front measured after focusing by a regen beam with no correction. rms, 0.936λ; peak-to-valley distance, 4.247λ. (b) Corrected wave-front after focusing by a regen beam. rms, 0.066λ; peak-to-valley distance, 0.618λ. (c) Differential wave front at 45 TW versus regen beam. rms, 0.154λ; peak-to-valley distance, 0.657λ. (d) Calculated focal intensity with no correction at full power (45 TW). $I_{\text{peak}} = 1 \times 10^{21}$ W/cm^2. (e) Calculated focal intensity after correction of the aberrations of the regen beam and the paraboloid. $I_{\text{peak}} = (6.9 \pm 0.7) \times 10^{21}$ W/cm^2. (f) Calculated focal intensity with the correction of the aberrations from power amplifiers. $I_{\text{peak}} = (1 \pm 0.1) \times 10^{22}$ W/cm^2.
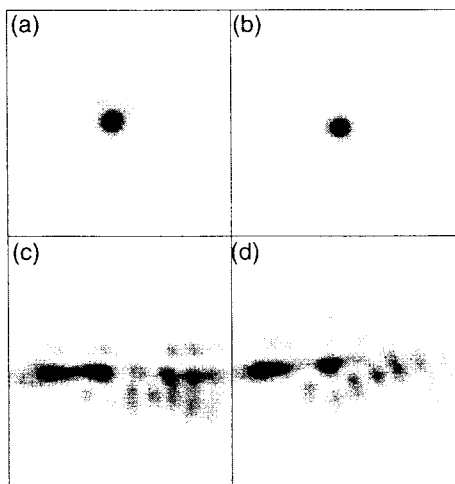
Fig. 3. (b), (d) Comparison of focal spot calculation and (a), (c) measurement with a 12-bit CCD camera at the regen level. (c), (d) Before correction; (a), (b) after correction. (b), (d) Calculated by use of measured phase and amplitude profile after focusing.

[Fig. 2(b)] and the differential phase. However, direct addition of the two fields is not possible owing to the field redistribution after parabolic reflection [see the spot diagrams in Fig. 1(a)]. Thus a transformation of coordinates is necessary for describing the field before and after reflection off the paraboloid. The transformation is given by

$$x_0 = 2f(-p \cos \varphi + m \sin \varphi)/(1 + p \sin \varphi + m \cos \varphi),$$

$$y_0 = 2f(-q)/(1 + p \sin \varphi + m \cos \varphi),$$

where f is the parent focal length of a paraboloid and p, q, and m [$=(1 - p^2 - q^2)^{1/2}$] are direction cosines viewed from the focus and can be considered coordinates of the reflected field. (x_0, y_0) are coordinates of the field before reflection across the beam near the paraboloid. φ is the mean incidence angle of the focusing beam (74.3°). After transformation of the differential phase in terms of the reflected field coordinates, the two phases were summed for diffraction calculation. The amplitude was also measured and taken into account. The diffraction integral used is derived for an off-axis paraboloid from the Stratton–Chu formula[4] with a far-field approximation. The far-field formulas satisfy all four of Maxwell's equations in vacuum. To calculate intensity, we consider only monochromatic diffraction; the finite pulse duration effect becomes significant only in the subcycle pulse regime.[9] Figures 2(d) and 2(e) show the calculated focused intensity distribution without any corrections and with correction of the aberrations in the regen beam and the paraboloid at 45 TW, and the peak intensities are 1×10^{21} and $(6.9 \pm 0.7) \times 10^{21}$ W/cm^2, respectively. The peak intensity can be further increased to $(1.0 \pm 0.1) \times 10^{22}$ W/cm^2 by correction of the differential phase at high energy [Fig. 2(f)]. The correction for the high-energy beam can be achieved by addition of the differential phase to the wave-front sensor measurements of the low-energy correction mode. This correction is possible only because of shot-to-shot wave-front stability. Thus the correction of the paraboloid and the low- and high-energy laser beam aberrations can be achieved through accurate measurement of the wave front.

We have demonstrated that by focusing a 45-TW laser beam to a spot size of 0.8 μm a record peak intensity of 1×10^{22} W/cm^2 can be reached. To obtain such a tight focus with an excellent Strehl ratio of 0.9 we use an $f/0.6$ paraboloid and correct it by a 96-actuator deformable mirror. Applications for such high intensity concentrated within one wavelength are the efficient generation of isolated attosecond pulses[10] and attosecond electron bunches.[11] The direct wave-front correction shown in this Letter is applicable only in a laser system that produces a stable shot-to-shot wave front. We have demonstrated a technique based on accurate wave-front measurement that can provide amplitude and phase information anywhere in the focal volume with high spatial resolution. We believe that the full characterization of a high-intensity beam will provide a new tool for accurately simulating experiments in this intensity regime. We believe that it will be possible to demonstrate an intensity of 10^{23} W/cm^2 following an upgrade of our laser system.

References

1. S. V. Bulanov, T. Zh. Esirkepov, J. Koga, and T. Tajima, Plasma Phys. Rep. 30, 196 (2004).
2. J. D. Bonlie, F. Patterson, D. Price, B. White, and P. Springer, Appl. Phys. B 70, S155 (2000).
3. F. Druon, G. Chériaux, J. Faure, J. Nees, M. Nantel, A. Maksimchuk, G. Mourou, J. C. Chanteloup, and G. Vdovin, Opt. Lett. 23, 1043 (1998).
4. P. Varga and P. Török, J. Opt. Soc. Am. A 17, 2081 (2000).
5. D. S. Montgomery, R. P. Johnson, H. A. Rose, J. A. Cobble, and J. C. Fernández, Phys. Rev. Lett. 84, 678 (2000).
6. P. Agostini, G. Barjot, J. F. Bonnal, G. Mainfray, C. Manus, and J. Morellec, IEEE J. Quantum Electron. QE-4, 667 (1968).
7. V. Yanovsky, S.-W. Bahk, C. Felix, N. Saleh, P. Rousseau, V. Chvykov, and G. Mourou, in Conference on Lasers and Electro-Optics (CLEO), Vol. 73 of OSA Trends in Optics and Photonics Series (Optical Society of America, Washington, D.C., 2002), paper CMK4.
8. Z. Sacks, G. Mourou, and R. Danielius, Opt. Lett. 26, 462 (2001).
9. B. Rau, T. Tajima, and H. Hojo, Phys. Rev. Lett. 78, 3310 (1997).
10. N. M. Naumova, J. A. Nees, I. V. Sokolov, B. Hou, and G. A. Mourou, Phys. Rev. Lett. 92, 063902 (2004).
11. N. M. Naumova, I. Sokolov, J. Nees, A. Maksimchuk, V. Yanovsky, and G. Mourou, "Attosecond electron bunches," Phys. Rev. Lett. (to be published).

Ultrafast Optics

Errata

Annual Indexes